MINIMAL GAIN MARCHING SCHEMES FOR STEADY-STATE SOLUTION GENERATION

Renan de Souza Teixeira, renanpcivil@yahoo.com.br

Programa de Pós-Graduação em Engenharia de Defesa - PGED,Instituto Militar de Engenharia - IME, Praça Gal. Tibúrcio n:80, Praia Vermelha, Rio de Janeiro, RJ 22290-270, Brazil

Leonardo S. de B. Alves, leonardo.alves@gmail.com

Departamento de Engenharia Mecânica, Universidade Federal Fluminense - UFF, Rua Passo da Pátria, 156, São Domingos, Niterói, RJ 24210-240, Brazil

Abstract. *Numerical simulations of free shear layer has a critical point in the definition of accurate initial and boundary conditions. Different explicit and implicit marching schemes are described in this current paper. This procedure can be applied in a existing code designed for unsteady simulations. The steady-state solution are obtained efficiently with a parameter θ of marching methods. Linear stability analysis is the fundamental theory that guarantee the optimal convergence in a process. This new methodology is tested on a code designed for compressible Navier-Stokes equation with arbitrary Mach number. Different θ are investigated to demonstrate the efficiency of the methodology. The optimal convergence was demonstrated for both methodologies.*

Keywords:*Implicit and explicit scheme, Numerical Stability Analysis, Arbitrary Mach number, Steady-State solution, Initial and Boundary Conditions.*

1. Introduction

Free shear flows are unbounded regions of a large body of fluid, which have either excess momentum, such as jet and mixing layer, or momentum deficit, like wake. This kind of flow have been the subject of extensive research over the past several decades, mostly because they have applications in many engineering fields. The development of the coherent structure formed by the mixing layer are responsible for control of the air-fuel mixture ratio in the primary zone of gas turbine combustors and pollution dispersion from chimneys into the atmosphere. Numerical studies of these flows help us to understand some important characteristics of their physics.

Spatially developing incompressible planar mixing layers represents a free shear layer that is already convectively unstable at very low Reynolds numbers. In such cases, small perturbations are amplified as they propagate downstream. The first coherent structure formed in a transient simulation is the start-up vortex. Many authors claim that a first derivative discontinuity between initial and inflow conditions is responsible for its formation (Buell and Huerre, 1988). Nevertheless, another studies show that numerical reflections provide from outlet conditions create a non-physical feedback effect (Teixeira, 2010; Teixeira and Alves, 2011). In the absence of external excitations, the flow should relax to its steady-state solution according to both linear (Ho and Huerre, 1984; Huerre and Monkewitz, 1990) and nonlinear studies (Chomaz, 2005). However, undesirable numerical reflections corrupt the simulation preventing the steady-state solution.

The small amount of computer simulations about this problem present in the literature can be seen in the article by McMullan *et al.* (2007), which simulates incompressible spatially developing planar mixing layers in two and three dimensions. The hyperbolic tangent function and data derived from boundary layer simulations are used to generate the inflow conditions, which are extended to the rest of the domain in order to form the respective initial conditions. They show important differences between each one of these cases, providing strong evidence that initial conditions must be as close as possible to the experiment they intend to reproduce for a good agreement to be possible.

The study of accurate initial conditions was developed for direct numerical simulation of temporal compressible binary shear layers (Lardjane *et al.*, 2004). The effects of the density ratio, convective Mach number and free streams temperature was illustrated for the different initial condition. The amplitude of early acoustic wave is strongly reduced due the accurate

initial condition. A novel numerical methodology to generate accurate initial conditions for unsteady simulations was presented in Teixeira and Alves (2012). In this method the physical-time damping with first-order backward difference formula (BDF) (Venkateswaran *et al.*, 2003) is introduced through a dual time stepping scheme to eliminate transient fluctuations without affecting spatial resolution. However, only simulations of low stiff test cases (velocity ratio ~ 2 or 4) were presented.

One of the critical points in the computer simulation of external flows is the appropriate implementation of initial and boundary conditions. A possible solution to this problem is coordinate transformation, i.e., mapping the unbounded domain into a bounded one before attempting a numerical solution of the respective governing equations (Grosch and Orszag, 1977). Two types of high accuracy artificial boundary conditions can be found in the literature. The first type includes global boundary conditions, which require a finite region that extends away from the boundary to be effective (Blaschak and Kriegsmann, 1988; Bodony, 2006). The other type includes local boundary conditions, which only act on the artificial boundary controlling the inflow and outflow of waves crossing it. One widely used subset is known as non-reflective boundary conditions. They model the behavior of linear perturbations around a reference solution at the boundary (Giles, 1990; Colonius *et al.*, 1993) in order to minimize reflections.

The following sections present a formulation of temporal derivative discretization that eliminate the transient fluctuations efficiently. This procedure is an extension of the methodology developed by Teixeira and Alves (2012). The density-based approach developed by Merkle and co-workers (Venkateswaran and Merkle, 2000; Buelow *et al.*, 2001) are employed in the current paper. The spatial derivatives were aproximated with central differences on a non-uniform mesh (Teixeira and Alves, 2010; Teixeira *et al.*, 2008), with matrix artificial dissipation applied for the inviscid fluxes (Medeiros and Alves, 2010; Medeiros, 2012).

2. Mathematical Model

Actually numerical methods have been the principal investigation instrument of the partial differential equation (PDE). Derivative approximations are used to discretize the original PDE (or system of PDEs). The method to approximate derivatives applied in this paper was the finite-difference method (Tannehill *et al.*, 1997). The mathematical model present here is based on treatment of the temporal derivatives of a system of PDEs like as

$$\frac{\partial \mathbf{Q}}{\partial t} = \mathbf{f}(\mathbf{Q}) \tag{1}$$

where $\mathbf{Q}$ is the variable vector.

The introduction report the difficult to obtain agreement initial and boundary conditions in free shear flows. A implicit Euler scheme generate reference solutions to mixing layer problem (Teixeira and Alves, 2012). In order to improve the efficiency to generate reference solutions we modify the implicit and explicit Euler schemes to introduce dissipative error and reach the convergence. A combination of two differences derivatives approximations control the spatial fluctuations (Zhong, 1998). In the explicit Euler scheme we apply a compounding of different discretization. The temporal derivative was discretized with a linear combination between backward and central difference approximations. It follows that the difference approximation to the first temporal derivative of a system of equations 1 can be written as

$$\frac{\partial \mathbf{Q}}{\partial t} = \theta \frac{\mathbf{Q}^{n+1} - \mathbf{Q}^{n}}{\Delta t} + (1-\theta)\frac{\mathbf{Q}^{n+1} - \mathbf{Q}^{n-1}}{2\Delta t} = \mathbf{f}(\mathbf{Q}^{n}) + E.T., \tag{2}$$

where θ is the dissipative control parameter, resulting in the following equation

$$\frac{\partial \mathbf{Q}}{\partial t} = \frac{(1+\theta)\mathbf{Q}^{n+1} - 2\theta\mathbf{Q}^{n} - (1-\theta)\mathbf{Q}^{n-1}}{2\Delta t} = \mathbf{f}(\mathbf{Q}^{n}) + E.T., \tag{3}$$

where the truncation error is described as

$$E.T. = \theta\frac{\Delta t}{2}\frac{\partial^2 Q}{\partial t^2} - \frac{\Delta t^2}{6}\frac{\partial^3 Q}{\partial t^3} + \theta\frac{\Delta t^3}{24}\frac{\partial^4 Q}{\partial t^4} - \frac{\Delta t^4}{120}\frac{\partial^5 Q}{\partial t^5} + \dots \tag{4}$$

whose the dissipative control parameter θ is associated to even derivatives. Thus, if we increase the θ the dissipative error must increase.

In the implicit scheme we applied the generalized Crank-Nicholson method (Anderson, 1995) with the same dissipative control parameter θ of the equation 2 can observed equation 5

$$\frac{\partial \mathbf{Q}}{\partial t} = \frac{\mathbf{Q}^{n+1} - \mathbf{Q}^n}{\Delta t} = \theta\mathbf{f}(\mathbf{Q}^{n+1}) + (1-\theta)\mathbf{f}(\mathbf{Q}^n) + E.T. \tag{5}$$

and the truncation error is

$$E.T. = (2\theta - 1)\frac{\Delta t}{2}\frac{\partial^2 Q}{\partial t^2} - (6\theta^2 - 6\theta + 1)\frac{\Delta t^2}{6}\frac{\partial^3 Q}{\partial t^3} + \dots \tag{6}$$

A system of ordinary differential equations (ODE) will be employed to certificate the method behavior. This one was implemented to improve the readers comprehension. On the other hand, the ODE 7 represent a good nonlinear problem to test our methodology due their chaotic characteristic. This system of equations was first formulated in 1963 by E. N. Lorenz and possesses what has come to known as a “strange attractor" (Hirsch *et al.*, 2004). The Lorentz equation is defined as

$$\begin{cases} \dfrac{dx}{dt} &= \sigma\,(y - x) \\ \dfrac{dy}{dt} &= \rho x - y - xz \\ \dfrac{dz}{dt} &= -\beta z + xy \end{cases} \tag{7}$$

where x, y and z are the independent variables, σ is the Prandtl number, ρ is the Rayleigh number and β is related to the physical size of the system.

The modified explicit Euler and generalized Crank-Nicholson methods are implemented in the above problem. The set of Lorentz problem constants are: $\sigma = 10$, $\beta = 8/3$ and $\rho = 18$. A investigation of different parameters θ is presented in Figure 1. The Figure 1 (left) show the convergence process of the Lorentz problem with modified explicit Euler scheme and the Figure 1 (right) show the convergence with the generalized Crank-Nicholson scheme. In both cases, the figure shows the number of physical-time iterations as the different physical-time steps Δt are performed. The different kind of lines shows the convergence towards steady-state for different parameters θ. The physical-time iterations were performed until the maximum absolute error of the residue's L2 norm was below $d\mathbf{x}/dt \leq 1.0 \times 10^{-08}$. The Figure 1 (left) show an optimal physical-time step Δt less than the maximum physical-time step Δt. However, the dissipative terms of the truncation error in the equations 4 and 6 are associated with the parameter θ and physical-time step Δt. Thus, it was expected the optimal convergence in maximum parameter θ and physical-time step Δt.

On the other hand, the implicit scheme case in Figure 1 (right) show a strange behavior. This should happen due the numeric nature of the problem. Then, a problem with more complexity must be employed. The linear stability analysis was employed to understand the error behavior of the proposed schemes.

Numerical Stability is a study of error behavior in a only marching numerical scheme. A stable numerical method is one the error not grow in the numerical procedures (Tannehill *et al.*, 1997). Particularly, in this current paper, we are looking for which manner the error diminish efficiently. The study display the gain as the different physical-time step Δt are performed. The Figure 2 shows the stability analysis of the modified explicit Euler scheme (left) and generalized

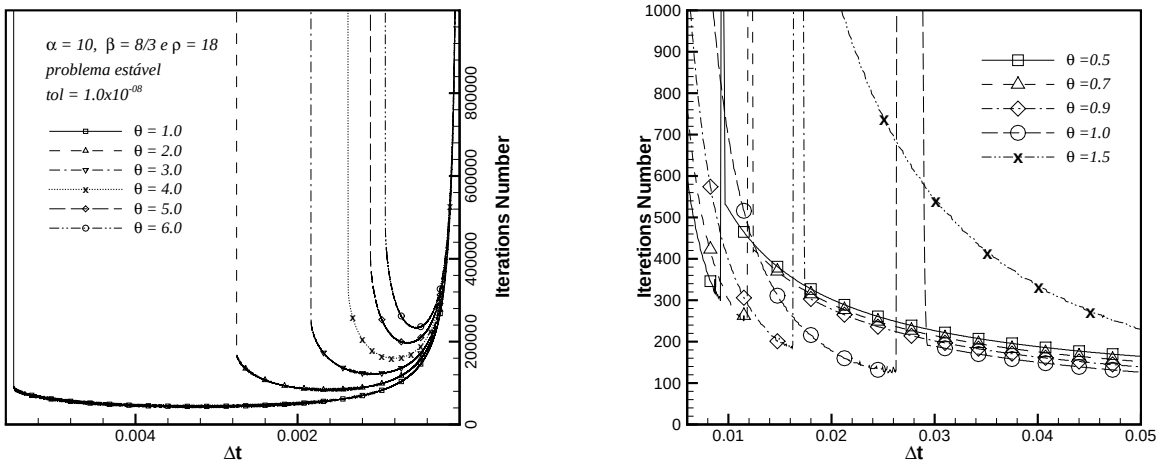

Figure 1. Steady-state convergence of Lorentz problem using modified explicit Euler scheme (left) and generalized Crank-Nicholson scheme (right) for different θ parameters.

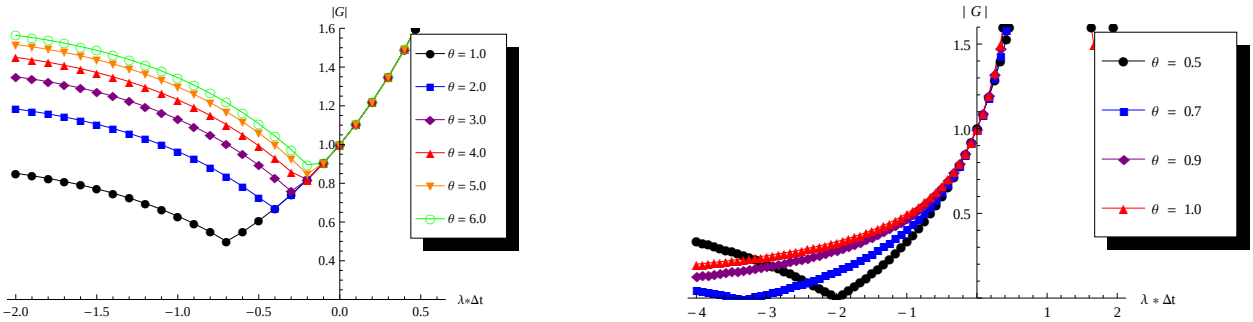

Figure 2. Linear stability analysis for modified explicit scheme (left) and implicit scheme (right).

Crank-Nicholson (right). In both figures each line color shows the stability analysis for different parameters θ. The region of minimal gain is evidence in explicit scheme analysis. For each θ parameter a existence of optimal physical-time step Δt can be observed in Figure 2 (left). The mentioned phenomena agrees with numerical result present in Figure 1 (left). However, the stability analysis for the implicit method of Figure 2 (right) just has a optimal physical-time step Δt for some specific parameters θ. For the implicit scheme analysis, the numerical studies has a good agreement with the stability analysis for small physical-time step Δt. Thus, the methodology of this research is about the optimal step time Δt for drive the solution towards steady-state regime. The following section present the preconditioned dual-time (DTS) procedures.

2.1 Dual-Time Step Procedure

Let's consider the compressible Navier-Stokes equations described in equation 1 where t is the physical time variable, $\mathbf{Q}$ is the conservative variable and $\mathbf{f}(\mathbf{Q})$ is the steady-state residue of purpose problem. When solving these equations numerically one has to use their discrete form. This one leads a significant problem when the Mach number approach zero, i.e. $M \to 0$. Thus, two different approaches must be used to solve one. Fist we solve the pressure field directly and decompose the pressure into a constant reference pressure p_0 and a gage pressure p_g , i.e., $p(x,t) = p_0 + p_g(x,t)$. Then, the equation 1 is rewritten as

$$\mathbf{T}\frac{\partial \hat{\mathbf{Q}}}{\partial t} = \mathbf{f}(\mathbf{Q}), \tag{8}$$

where $\mathbf{T} = \partial\mathbf{Q}/\partial\hat{\mathbf{Q}}$ is the vector to modify the conservative to primitive variables and $\hat{\mathbf{Q}}$ is the primitive variable vector that includes the gage pressure, all velocities components and temperature. The equation 8 can not be used if the Mach number is less than $M \sim 0.1$. However, minor values for Mach number can be achieved with the second approach, knowledge as preconditioning for low Mach number (Turkel, 1993, 1999). This is possible with the substitution of the Jacobian $\mathbf{T}$ by the preconditioned matrix $\mathbf{\Gamma}$, where we obtain the preconditioned equations

$$\mathbf{\Gamma}\frac{\partial\hat{\mathbf{Q}}}{\partial\tau} = \mathbf{f}(\mathbf{Q}), \tag{9}$$

where τ is the pseudo-time independent variable. Indeed, the preconditioned matrix Γ is the modified Jacobian $\mathbf{T}$ that the eigenvalues of the equation 8 have the same order of magnitude (Turkel, 1987). Nevertheless, this procedure alters the original physical-time t, therefore the pseudo time becomes the new marching variable. This process accelerate the convergence of the original system, 1 or 8, towards steady-state. The solution $\mathbf{f}(\mathbf{Q}) = 0$ of the original system in the limit $t \to \infty$ is the same of equation 9 in the limit $\tau \to \infty$.

Introducing the original physical time derivative in equation 9, the unsteady problem can be evaluated, because of this we have

$$\mathbf{\Gamma}\frac{\partial\hat{\mathbf{Q}}}{\partial\tau} + \frac{\partial\mathbf{Q}}{\partial t} = \mathbf{f}(\mathbf{Q}), \tag{10}$$

where this procedure is knowledge as dual-time step method (DTS) (Merkle and Choi, 1988). Once the steady-state solution is obtained in each physical time step the original government equation 1 is recovered, since $\partial\hat{\mathbf{Q}}/\partial\tau \simeq 0$ in this limit.

The approach traditionally used to solve the equation 10 considers the physical-time derivative as a source term, where we obtain

$$\mathbf{\Gamma}\frac{\partial\hat{\mathbf{Q}}}{\partial\tau} = \mathbf{f}(\mathbf{Q}) - \frac{\partial\mathbf{Q}}{\partial t}, \tag{11}$$

where a multi-step scheme can be employed (Alves, 2009). Because of two different time derivative the time derivative discretization presented in the last section can be applied in both time derivative. Initially, the explicit scheme is presented. Thus, using the explicit scheme of equation 3 in the physical-time derivative the equation 11 becomes

$$\mathbf{\Gamma}^p\frac{\partial\hat{\mathbf{Q}}}{\partial\tau} = \mathbf{f}(\mathbf{Q}^n) - \frac{(1+\theta_1)\mathbf{Q}^{n+1} - 2\theta_1\mathbf{Q}^n - (1-\theta_1)\mathbf{Q}^{n-1}}{2\Delta t}. \tag{12}$$

When we apply the modified explicit method in the pseudo time derivative it is important to assume dependent unknown variables in physical $(n+1)$ and pseudo $(p+1)$ time are equal. This approximation is necessary to employ the multi-step marching scheme (Turkel and Vatsa, 2005). Thus, the equation 12 is given by

$$\mathbf{\Gamma}^p\frac{(1+\theta_2)\hat{\mathbf{Q}}^{p+1} - 2\theta_2\hat{\mathbf{Q}}^p - (1-\theta_2)\hat{\mathbf{Q}}^{p-1}}{2\Delta\tau} = \mathbf{f}(\mathbf{Q}^n) - \frac{(1+\theta_1)\mathbf{Q}^{p+1} - 2\theta_1\mathbf{Q}^n - (1-\theta_1)\mathbf{Q}^{n-1}}{2\Delta t}. \tag{13}$$

such organizing the equation 13 in residual form, we have

$$(1+\theta_2)\frac{\mathbf{\Gamma}^p}{2\Delta\tau}\Delta\hat{\mathbf{Q}} = \frac{(\theta_2-1)}{2\Delta\tau}\left(\hat{\mathbf{Q}}^p - \hat{\mathbf{Q}}^{p-1}\right) + \mathbf{f}(\mathbf{Q}^n) - \frac{(1+\theta_1)\mathbf{Q}^{p+1} - 2\theta_1\mathbf{Q}^n - (1-\theta_1)\mathbf{Q}^{n-1}}{2\Delta t}, \tag{14}$$

where $\Delta\hat{\mathbf{Q}} = \hat{\mathbf{Q}}^{p+1} - \hat{\mathbf{Q}}^p$.

Finally, after linearizing equation 14 in pseudo-time, we obtain the equation for discretized modified explicit scheme

$$\left\{(1+\theta_2)\frac{\mathbf{\Gamma}}{2\Delta\tau} + (1+\theta_1)\frac{\mathbf{T}}{2\Delta t}\right\}^p \Delta\hat{\mathbf{Q}} = \frac{(\theta_2-1)}{2\Delta\tau}\left(\hat{\mathbf{Q}}^p - \hat{\mathbf{Q}}^{p-1}\right) + \mathbf{f}(\mathbf{Q}^n) - \frac{(1+\theta_1)\mathbf{Q}^p - 2\theta_1\mathbf{Q}^n - (1-\theta_1)\mathbf{Q}^{n-1}}{2\Delta t}.$$

(15)

Now we present the equation 11 with generalized Crank-Nicholson in both temporal derivatives. Initially, the implicit scheme is applied in physical-time derivative. The equation 11 becomes

$$\mathbf{\Gamma}^p \frac{\partial \hat{\mathbf{Q}}}{\partial \tau} = \widetilde{\mathbf{f}}(\mathbf{Q}) = \theta_1 \mathbf{f}(\mathbf{Q}^{n+1}) + (1-\theta_1)\mathbf{f}(\mathbf{Q}^n) - \frac{\mathbf{Q}^{n+1} - \mathbf{Q}^n}{\Delta t}. \tag{16}$$

applying the generalized Crank-Nicholson scheme to march equation 16 in pseudo-time leads to

$$\mathbf{\Gamma}^p \frac{\hat{\mathbf{Q}}^{p+1} - \hat{\mathbf{Q}}^p}{\Delta \tau} = \theta_2 \widetilde{\mathbf{f}}(\mathbf{Q}^{p+1}) + (1-\theta_2)\widetilde{\mathbf{f}}(\mathbf{Q}^p) \tag{17}$$

linearizing the unknown terms in pseudo-time we have

$$\left\{ \frac{\mathbf{\Gamma}}{\Delta \tau} - \theta_2 \frac{\partial \widetilde{\mathbf{f}}(\mathbf{Q})}{\partial \hat{\mathbf{Q}}} \right\}^p \Delta \hat{\mathbf{Q}} = \widetilde{\mathbf{f}}(\mathbf{Q}^p) \tag{18}$$

where $\partial \widetilde{\mathbf{f}} / \partial \hat{\mathbf{Q}}$ includes the inviscid and transient Jacobians with the primitive variable vector $\hat{\mathbf{Q}}$ and $\hat{\mathbf{Q}}^{p+1} = \hat{\mathbf{Q}}^p + \Delta \hat{\mathbf{Q}}$. Combining equations 18 and 17 yields

$$\left\{ \frac{\mathbf{\Gamma}}{\Delta \tau} - \theta_2 \left(\frac{\mathbf{T}}{\Delta t} + \theta_1 \frac{\partial \mathbf{f}}{\partial \hat{\mathbf{Q}}} \right) \right\}^p \Delta \hat{\mathbf{Q}} = \theta_1 \mathbf{f}(\mathbf{Q}^p) + (1-\theta_1)\mathbf{f}(\mathbf{Q}^n) - \frac{\mathbf{Q}^p - \mathbf{Q}^n}{\Delta t}, \tag{19}$$

where $\partial \mathbf{f} / \partial \hat{\mathbf{Q}}$ contains the inviscid Jacobians.

3. Results and Discussions

The one-dimensional compressible Navier-Stokes equation is solved by numerical method. According the perturbation theory, compressible flows can keep three types of disturbance: entropic waves, vorticity and sound. This one are independent if their fluctuations are small, otherwise the disturbance will interact. Then, small density fluctuations just will be convected in a streamwise direction without any amplitude, frequency and phase variation. In this research, the entropic waves was simulated constant at low Mach number flow. The one is generated by a density disturbance with constant velocity and pressure. The temperature variations are obtained from state equation. If the initial condition is an arbitrary dimensional functions $f(x)$ for density its transient behavior will be defined by $\rho(x,t)/\rho_0 = f(x - u_0 t)$. The initial condition is defined as

$$f(x) = 1 + \delta_0 \sin(2\pi x / l_0), \qquad \text{with} \qquad 0 \leq x \leq l_0, \tag{20}$$

where ρ_0 and u_0 is the mean density and velocity, where the Mach number is $M = 10^{-3}$, δ_0 is the amplitude, l_0 is the wavelength and $t_0 = l_0/u_0$ period of perturbation. The reference pressure and temperature are $P_0 = 101325Pa$ and $T_0 = 300K$.

First of all, the impact of the methodology on the pseudo-time derivative was investigated. The Figure 3.show the number of iterations for different pseudo-time step $\Delta\tau$ in the case of modified explicit Euler method (left) and generalized Crank-Nicholson method (right). In the physical-time was employed the Crank-Nicholson scheme with twenty points per period. In both cases, each type of line show the iterations number in pseudo-time step in the first physical-time step for different parameter θ. According to linear stability analysis, the Figure 3.(left) show a region of optimal pseudo-time step $\Delta\tau$ different of maximum one. On the other hand, the Figure 3.(right) shows an optimal pseudo-time step $\Delta\tau$ only for some parameters θ. This results evidence the good agreement with stability analysis.

Now that the study of physical marching schemes have been illustrated in pseudo-time, an evaluation of the two

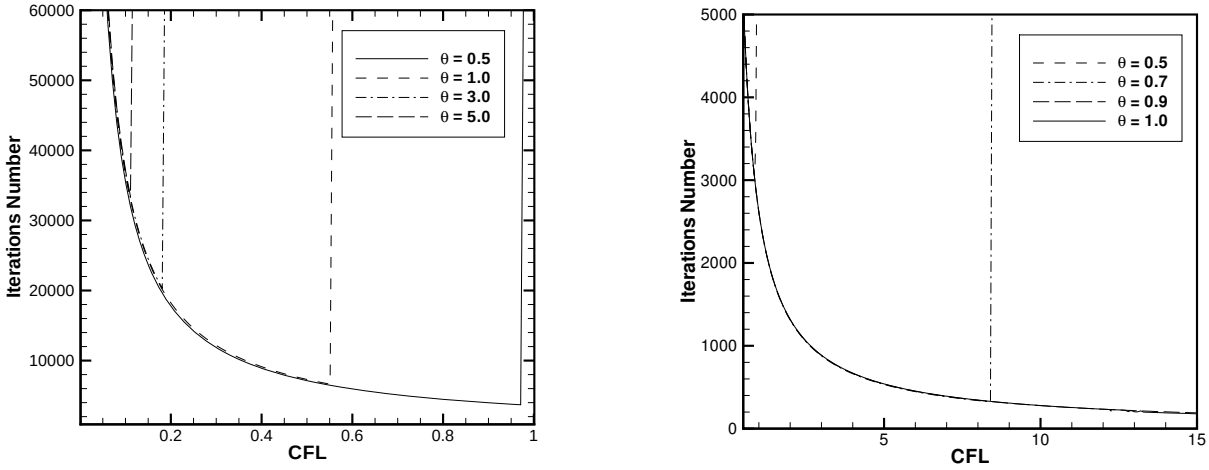

Figure 3. Number of iterations for different pseudo-time step $\Delta\tau$ for modified explicit scheme (left) and implicit scheme (right)

physical damping models in physical-time is presented. The Figures 4 and 5 show the convergence to artificial steady-state solution for different CFL number ($CFL = \Delta t \cdot u_0/l_0$). A tolerance ($\Delta\mathbf{Q}/\Delta t < 10^{-8}$) was imposed to reach the steady-state. Different parameters θ was investigated for both methods. The iterations number for each physical-time step for the Modified Explicit Euler scheme is presented. The total iterations number in pseudo-time is given to show the existence of a optimal CFL for each parameter θ.

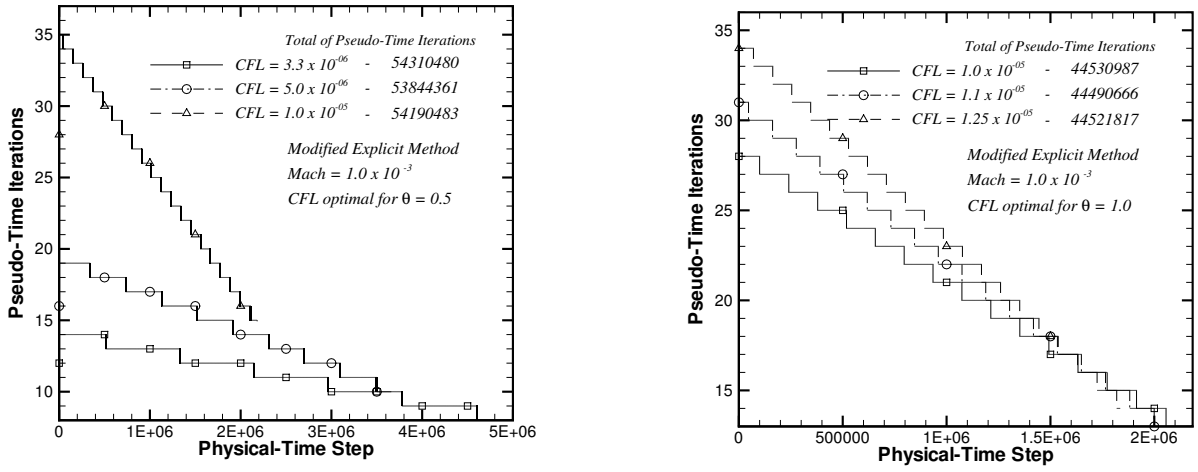

Figure 4. Pseudo-time iterations and steady-state convergence in physical-time for Modified Explicit Euler scheme.

In the Figure 4 the convergence for the Modified Explicit Euler method is presented. The Modified Explicit Euler scheme was employed in pseudo-time derivative with $\theta = 0.5$. The Figure 4 (left) illustrate the case with $\theta = 1.0$ and Figure 4 (right) the case with $\theta = 0.5$. In both cases, the existence of a optimal CFL is evidence and a similar behavior is observed for a wide range of parameters ($0.3 \leq \theta \leq 2.0$). The Figure 4 describes the accelerate convergence with the θ variation, i. e., when increase the parameter the total iterations number in the pseudo-time decrease and the total steps in physical-time also decrease.

On the other hand, in Figure 5 the convergence for the Generalized Crank-Nicholson method is presented. In the

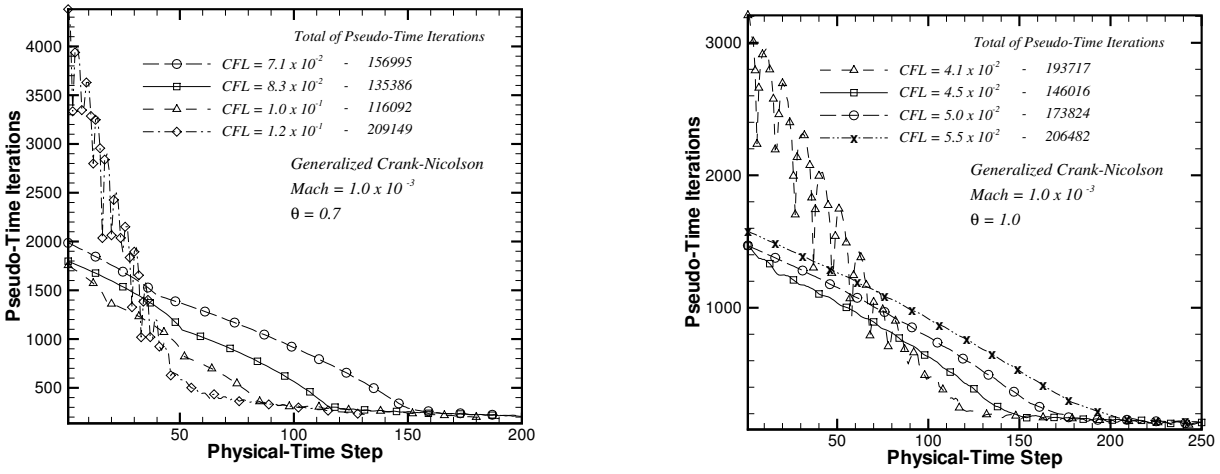

Figure 5. Pseudo-time iterations and steady-state convergence in physical-time for Generalized Crank-Nicholson scheme.

pseudo-time the convectional Crank-Nicholson scheme was employed. The Figure 5 (left) shows the convergence for the case which $\theta = 0.7$ and in the Figure 5 (right) illustrates the convergence progress for $\theta = 1.0$. The optimal CFL is observed for both cases of parameters θ. A wide range parameter was studied ($0.3 \leq \theta \leq 2.5$). The similar behavior was observed. A good agreement with the linear stability analysis was demonstrated for two methods. The iterations number in pseudo-time for each physical-time step for Modified Explicit method is 0.7% of Generalized Crank-Nicholson. However, the Modified Explicit Euler schemes required a high computational cost, i. e., the number of steps in physical-time to reach convergence, is 25000 times greater than implicit one. According the region stability of explicit scheme the CFL number is lower. So, optimal CFL for this one gives the total iterations number in pseudo-time 21% higher than implicit scheme. This results suggest in unstable problems the explicit scheme is unavailable.

4. Conclusions and Future Works

The current paper showed, in the present literature, that several of the most accurate compressible flow employed today has the difficult to describe the initial and boundary conditions. The physical-time damping was described as a good procedure to generate a steady-state solution (Teixeira and Alves, 2011). It can be easily applied to any existing unsteady flow code. The modifications in physical marching schemes can accelerate the convergence and give a optimal convergence process, based on linear stability analysis. The results illustrate the existence of a CFL optimal for each methods. The computational cost was 400 times greater in Explicit scheme.

The study in a 2D compressible unsteady flow will employ. Future work will test this procedure on more challenging problems as well as utilize such steady-states as initial and boundary conditions which require reference solutions.

5. ACKNOWLEDGEMENTS

The authors would like to acknowledge the financial support of CAPESBrazil and Instituto Militar de Engenharia (IME).

6. REFERENCES

Alves, L.S.B., 2009. "Review of numerical methods for the compressible flow equations at low mach numbers". In *XII Encontro de Modelagem Computacional*. Rio de Janeiro, RJ, Brazil.

Anderson, J.D., 1995. *Computational Fluid Dynamics: The Basic with Applications*. MacGraw Hill, Inc., New York.

Blaschak, J.G. and Kriegsmann, G.A., 1988. "A comparative study of absorbing boundary conditions". *Journal of Computational Physics*, Vol. 77, pp. 109–139.

Bodony, D.J., 2006. "An analysis of sponge zones for computational fluid mechanics". *Journal of Computational Physics*, Vol. 212, No. 2, pp. 681–702.

Buell, J.C. and Huerre, P., 1988. "Inflow/outflow boundary conditions and global dynamics of spatial mixing layers". Technical Report N89–24540, Stanford University.

Buelow, P.E.O., Venkateswaran, S. and Merkle, C.L., 2001. "Stability and convergence analysis of implicit upwind schemes". *Computers and Fluids*, Vol. 30, pp. 961–988.

Chomaz, J.M., 2005. "Global instabilities in spatially developing flows: Non-normality and nonlinearity". *Annual Review of Fluid Mechanics*, Vol. 37, pp. 357–392.

Colonius, T., Lele, S.K. and Moin, P., 1993. "Boundary conditions for direct computation of aerodynamic sound generation". *AIAA Journal*, Vol. 31, No. 9, pp. 1574–1582.

Giles, M.B., 1990. "Nonreflecting boundary conditions for euler equation calculations". *AIAA Journal*, Vol. 28, No. 12, pp. 2050–2058.

Grosch, C.E. and Orszag, S.A., 1977. "Numerical solution of problems in unbounded regions: Coordinate transforms". *Journal of Computational Physics*, Vol. 25, pp. 273–296.

Hirsch, M.W., Smale, S. and Devaney, R.L., 2004. *Differential Equations, Dynamical Systems, and an Introduction to Chaos*. Academic Press Inc.

Ho, C.M. and Huerre, P., 1984. "Perturbed free shear layers". *Annual Review of Fluid Mechanics*, Vol. 16, pp. 365–424.

Huerre, P. and Monkewitz, P.A., 1990. "Local and global instabilities in spatially developing flows". *Annual Review of Fluid Mechanics*, Vol. 22, pp. 473–537.

Lardjane, N., Fedioun, I. and Gokalp, I., 2004. "Accurate initial conditions for the direct numerical simulation of temporal compressible binary shear layers with high density ratio". *Computers & Fluids*, Vol. 33, pp. 549–576.

McMullan, W.A., Gao, S. and Coats, C.M., 2007. "A comparative study of in?ow conditions for two- and three-dimensional spatially developing mixing layers using large eddy simulation." *International Journal for Numerical Methods in Fluids*, Vol. 55, pp. 589–610.

Medeiros, F.E.L., 2012. *Metodologia para o Desenvolvimento de Pre-Condicionadores Aplicados na Solucao de Escoamentos Compressiveis com Baixo Numero de Mach em Sistemas de Misseis e Foguetes.* Ph.D. thesis, Instituto Militar de Engenharia, Rio de Janeiro, Brazil.

Medeiros, F.E.L. and Alves, L.S.B., 2010. "Preconditionig methods for low mach number flow simulations with an optmized pseudo speed of sound." *13th Brazilian Congress of Thermal Engineering and Sciences*.

Merkle, C.L. and Choi, Y.H., 1988. "Computation of low speed compressible flows with time-marching methods". *International Journal for Numerical Methods in Engineering*, Vol. 25, pp. 293–311.

Tannehill, J.C., Anderson, D.A. and Pletcher, R.H., 1997. *Computational Fluid Mechanics and Heat Transfer*. Taylot & Francis, Philadelphia.

Teixeira, R.S., 2010. *Análise de Condições Iniciais e de Contorno na Simulação Computacional de Camadas de Mistura Planas*. Master's thesis, Intituto Militar de Engenharia, Rio de Janeiro.

Teixeira, R.S. and Alves, L.S.B., 2010. "A study of initial and boundary conditions for spatially developing planar mixing layers." *13th Brazilian Congress of Thermal Engineering and Sciences*.

Teixeira, R.S. and Alves, L.S.B., 2011. "Self-excited compressible planar mixing layer at arbitrary mach numbers: Numerical or physical phenomena?" In *21st International Congress of Mechanical Engineering*. Natal, RN, Brazil.

Teixeira, R.S. and Alves, L.S.B., 2012. "Modelling far-field entrainment in compressible flows". *International Journal of Computational Fluid Dynamics*, Vol. 26, pp. 67 – 78. doi:10.

Teixeira, R.S., Alves, L.S.B., Karagozian, A.R. and Kelly, R.E., 2008. "On the solution of the compressible flow equations at small mach numbers". In *12th Brazilian Congress of Thermal Engineering and Sciences*. Belo Horizonte, MG, Brazil.

Turkel, E., 1987. "Preconditioned methods for solving the incompressible and low speed compressible equations". *Journal of Computational Physics*, Vol. 72, No. 2, pp. 277–298.

Turkel, E., 1993. "Review of preconditioning methods for fluid dynamics". *Applied Numerical Mathematics*, Vol. 12, pp. 257–284.

Turkel, E., 1999. "Preconditioning techniques in computational fluid dynamics". *Annual Review of Fluid Mechanics*, Vol. 31, pp. 385–416.

Turkel, E. and Vatsa, V.N., 2005. "Local preconditioners for steady and unsteady flow applications". *ESAIM: Mathematical Modelling and Numerical Analysis*, Vol. 39, No. 3, pp. 515–535.

Venkateswaran, S. and Merkle, C.L., 2000. "Efficiency and accuracy issues in contemporary cfd algorithms". In *AIAA Conference Paper*. 2000-2251, pp. 1–16.

Venkateswaran, S., Merkle, C.L., Zeng, X.Q. and Li, D., 2003. "Influence of large scale pressure changes on preconditioning solutions at low speeds". In *AIAA Conference Paper*. 2003-3703.

Zhong, X., 1998. "High-order finite-difference schemes for numerical simulation of hypersonic boundary-layer transition". *Journal of Computational Physics*, Vol. 144, pp. 662–709.

7. RESPONSIBILITY NOTICE

The author(s) is (are) the only responsible for the printed material included in this paper.